Wiley Online Library
Early View publication on www.wileyonlinelibrary.com
(issue and page numbers not yet assigned;
citable using Digital Object Identifier – DOI)

J. Biophotonics 1–9 (2016) / **DOI** 10.1002/jbio.201600122

Journal of BIOPHOTONICS

FULL ARTICLE

Three-dimensional mapping of the orientation of collagen corneal lamellae in healthy and keratoconic human corneas using SHG microscopy

Raffaella Mercatelli[1], *Fulvio Ratto*[2], *Francesca Rossi*[2], *Francesca Tatini*[2], *Luca Menabuoni*[3], *Alex Malandrini*[3], *Riccardo Nicoletti*[4], *Roberto Pini*[2], *Francesco Saverio Pavone*[1, 5, 6], *and Riccardo Cicchi*[*, 1, 5]

[1] National Institute of Optics, National Research Council (INO-CNR), Via Nello Carrara 1, 50019 Sesto Fiorentino, Italy
[2] Institute of Applied Physics "N. Carrara" (IFAC-CNR), Via Madonna del Piano 10, 50019 Sesto Fiorentino, Italy
[3] U.O. Oculistica Nuovo Ospedale S. Stefano, Via Suor Niccolina Infermiera 20, 59100 Prato, Italy
[4] C.S.O S.r.l, Via degli Stagnacci 12/e, 50018 Scandicci, Italy
[5] European Laboratory for Non-Linear Spectroscopy (LENS), Via Nello Carrara 1, 50019, Sesto Fiorentino, Italy
[6] Department of Physics, University of Florence, Via G. Sansone 1, 50019 Sesto Fiorentino, Italy

Received 26 April 2016, revised 7 June 2016, accepted 7 June 2016
Published online 1 August 2016

Key words: Second-Harmonic Generation (SHG) microscopy, collagen, cornea, keratoconus

Keratoconus is an eye disorder that causes the cornea to take an abnormal conical shape, thus impairing its refractive functions and causing blindness. The late diagnosis of keratoconus is among the principal reasons for corneal surgical transplantation. This pathology is characterized by a reduced corneal stiffness in the region immediately below Bowman's membrane, probably due to a different lamellar organization, as suggested by previous studies. Here, the lamellar organization in this corneal region is characterized in three dimensions by means of second-harmonic generation (SHG) microscopy. In particular, a method based on a three-dimensional correlation analysis allows to probe the orientation of sutural lamellae close to the Bowman's membrane, finding statistical differences between healthy and keratoconic samples. This method is demonstrated also in combination with an epi-detection scheme, paving the way for a potential clinical ophthalmic application of SHG microscopy for the early diagnosis of keratoconus.

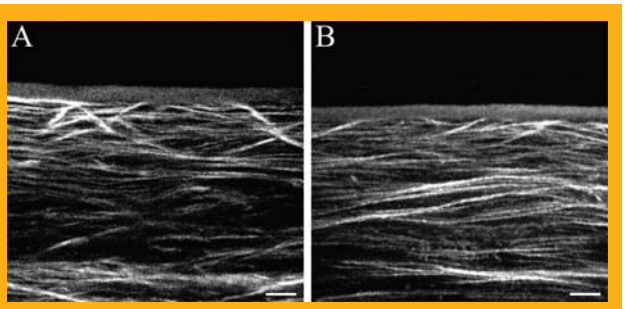

SHG image acquired with sagittal optical sectioning (**A**) of a healthy cornea and (**B**) of a keratoconic cornea. Scale bars: 30 μm.

* Corresponding author: e-mail: riccardo.cicchi@ino.it, Phone: +39 055 2308 228

Journal of BIOPHOTONICS

1. Introduction

The application of Non-Linear Optical (NLO) microscopy techniques in biological and medical fields has increased exponentially in the last two decades [1–3]. In fact, their unique features, such as intrinsic optical sectioning and deep imaging capability inside turbid media, make NLO-microscopy techniques particularly suitable for both *in vivo* and *ex vivo* imaging of biological tissues [4–7]. Among NLO microscopy techniques, Second-Harmonic Generation (SHG) microscopy is particularly useful for detecting non-centrosymmetric biological structures with high hyperpolarizability [8–10], like muscle fibres [11], microtubules [12] and collagen [13]. SHG microscopy offers several advantages, including large optical contrast, due to its inherent zero-background profile, and very low photo-toxic effects because electronic transfer phenomena are not involved in the optical process [14].

Cornea is an ideal target sample for SHG microscopy [15, 16] because it is a biological tissue largely composed of parallel collagen fibres that are arranged in stromal lamellae with typical sizes in the range of 10–230 μm in width, and 0.2–2.5 μm in thickness [17]. The suitability of SHG microscopy for probing the organization of corneal collagen lamellae has been already demonstrated in several studies, using both "en-face" [18–20] and sagittal optical sectioning geometry [21, 22], as well as using Polarization SHG (PSHG) [23, 24]. Recent studies have highlighted that healthy human cornea exhibits a population of collagen lamellae that insert into Bowman's membrane with an oblique orientation, rather than running parallel to the membrane itself [25, 26]. This particular type of lamellae, which are located immediately below Bowman's membrane and are inserting in the membrane itself, are called sutural lamellae. It seems that the oblique orientation of sutural lamellae with respect to the Bowman's membrane gives mechanical strength to the corneal tissue and is responsible for corneal stiffness [26–28]. Keratoconus is an eye disorder that features a decrease of stiffness in the central portion of the cornea, which takes a conical shape, thus impairing visual capabilities [29]. In keratoconus, sutural lamellae have been observed to be oriented at smaller angles with respect to Bowman's membrane [30], as compared to healthy cornea, probably jeopardizing the stiffness of central cornea. SHG imaging of cornea allows to visualize collagen lamellae with a very high signal-to-noise ratio [31] and to measure the orientation of sutural lamellae [32], if used in combination with sagittal optical sectioning geometry. The drawback of sagittal optical sectioning is that this geometry is prevented *in vivo*, so that this method is useful only if implemented for *ex vivo* imaging applications.

In this study, we implemented a method for measuring the inclination of sutural lamellae using z-stacks of SHG images acquired with "en-face" optical sectioning and epi-detection geometry. A cross-correlation analysis, performed both along the axial direction and within the radial plane allowed to determine the inclination angle of sutural lamellae with respect to the Bowman's membrane. This parameter turned out to correlate well with the morphology of both healthy and keratoconic corneas. In fact, a smaller inclination of sutural lamellae was found in keratoconus compared to healthy cornea, in agreement with previous studies. In addition, the proposed approach bypasses the time-consuming 3D image acquisitions and processing from large portions of cornea. Considering the fact that the "en-face" optical sectioning geometry with epi-detection is compatible with *in vivo* clinical imaging, the proposed method really holds the potential to be implemented for the early diagnosis of keratoconus in the ophthalmic clinic.

2. Materials and methods

2.1 Samples preparation

Pathological corneas affected by keratoconus were harvested from patients undergoing penetrating keratoplasty at the Department of Ophthalmology of the Nuovo Ospedale Santo Stefano (Prato, Italy). Keratoconic corneas were trephined with a femtosecond laser and soaked into a tissue preservation solution (Carry C, AL.CHI.MI.A. Srl, Padova, Italy) immediately after trephination [33, 34]. Imaging of these samples was performed within 24 hours from excision. Healthy corneas were provided by the Tuscan Eye Bank and selected among those not suitable for transplantation. They were stored in the same tissue preservation solution and imaged within 48 hours from delivery. This study was approved by the local ethical committee of the Santo Stefano hospital (Prato, Italy) and conducted in accordance with the tenets of the Declaration of Helsinki. The study included two healthy and two keratoconic corneas. The central portions (about 8 mm × 2 mm) of these samples were used for both sagittal and "en-face" SHG imaging.

2.2 SHG imaging setup

Human corneas were imaged using a custom-made laser-scanning non-linear microscope. Laser excitation is provided by a mode-locked Ti : Sapphire laser

(Mira 900 F, Coherent Inc., Santa Clara, CA, US) pumped by a frequency-doubled Nd:YVO_4 laser system, emitting at 532 nm (Verdi V10, Coherent Inc., Santa Clara, CA, US). The emission wavelength can be tuned in the range 700–980 nm, with a typical pulse duration of 130 fs and a repetition rate of 76 MHz. For SHG imaging, the excitation wavelength was tuned to 840 nm. Laser power was adjusted using a system made with a rotating half waveplate and a polarizer. Polarization was made circular on the sample, by means of a quarter waveplate inserted in the laser path and properly oriented for compensating unwanted polarization ellipticity introduced by optics. The excitation path includes also two galvanometric mirrors for raster scanning (VM500, GSI Lumonics, Karlsruhe, Germany), a beam expander and a water-immersion objective XLUM 20× (NA 0.9, WD 2 mm, Olympus Corporation, Tokyo, Japan). Backward-emitted SHG was collected by the same objective lens, reflected by a dichroic mirror 685DCXRU (Chroma Technology Corporation, Rockingham, VT, US) and directed into a photomultiplier tube H7422 (Hamamatsu, Hamamatsu City, Japan). Forward-emitted SHG was collected by a second water immersion objective lens Fluor 40× (NA 0.8, WD 2 mm, Nikon Corporation, Tokyo, Japan), reflected by a dichroic mirror 685DCXRU (Chroma Technology Corporation, Rockingham, VT, USA) and detected using a second photomultiplier tube H7422 (Hamamatsu, Hamamatsu City, Japan). Two narrow band-pass filters with a spectral characteristic centred at 420 ± 10 nm HQ420BP (Chroma Technology Corporation, Rockingham, VT, US) are placed in front of the photomultipliers in order to selectively detect second-harmonic light.

2.3 Image acquisition and analysis

SHG images, collected according to a sagittal optical sectioning geometry (focal plane perpendicular to the corneal surface) from the central portion of the corneal stroma, were acquired with a pixel dwell time of 20 µs, a field of view of 400 × 400 µm^2 and a resolution of 512 × 512 pixels^2 in both healthy and keratoconic corneas, using circular polarization. Only a backward detection scheme was used in these acquisitions. FFT analysis on sagittal optically sectioned SHG images was performed by selecting an area below Bowman's membrane corresponding to a stromal layer about 30 µm thick. This analysis included a total of 81 ROIs (400 × 30 µm^2) for healthy corneas, and 97 ROIs (400 × 30 µm^2) for keratoconic corneas. The aspect ratio R (the ratio between minor and major axis of the elliptic FFT profile) of the 2D-FFT plot was taken as an indicator of anisotropy. R was calculated according to the method described in [35].

SHG images and stacks, collected with "en-face" optical sectioning geometry, were acquired with a pixel dwell time of 20 µs, a field of view of 240 × 240 µm^2, and a resolution of 512 × 512 pixels^2 in both healthy and keratoconic corneas, using circular polarization. Both forward and backward detection schemes were used in these acquisitions. Each stack contained 15 images acquired from the Bowman's membrane down to a depth of 30 µm into the stroma, with axial steps of 2 µm. 3D reconstructions were obtained from these stacks by means of ImageJ (National Institutes of Health, Bethesda, VA, US) "Orthogonal Views" plugin. A custom analysis routine written in LabVIEW (National Instrument, Austin, TX, US) environment allowed to estimate the mean inclination angle of sutural lamellae that are visible in these stacks. Briefly, each acquired stack was divided into domains of radial size of 20 × 20 µm^2 and axial size of 30 µm. At first, the mean intensity $I_M(i)$ was calculated by averaging the measured SHG intensity over all axial images acquired within the domain i. Then, $I_M(i)$ was used as a threshold, so that pixel values below $I_M(i)$ were set to zero in each axial image. Finally, the axial Pearson cross-correlation [36] was computed and its half-decay length $C_Z(i)$ was evaluated in each domain i. The parameter $C_Z(i)$ represented the axial cross-correlation value.

In a similar way with respect to the axial one, radial Pearson cross-correlation was calculated in each axial image. Then, only radial cross-correlation values obtained from images comprised within a sub-stack, made of a number of axial images corresponding to the axial cross-correlation decay length divided by the axial step, were considered for the calculation. The cross-correlation values were calculated independently for the two orthogonal radial axes (x and y) and the radial half-decay length $C_M(i, z)$ was calculated as the root mean square of the x and y values in each image. Finally, a radial correlation length value $C_M(i)_{\mathrm{mean}}$ was then obtained for each domain by taking the average of the obtained values within the corresponding sub-stack. In this way, each domain was characterized by a typical axial $C_Z(i)$ and a typical radial $C_M(i)_{\mathrm{mean}}$ cross-correlation lengths. On the basis of these two values, an angle defined as follows:

$$\theta(i) = \mathrm{arctg}\,[C_Z(i)/C_M(i)_{\mathrm{mean}}] \quad (1)$$

was associated to each domain i. The parameter $\theta(i)$ was taken as an indicator of the average orientation of sutural lamellae with respect to the Bowman's membrane within each domain. Such parameter was then represented in a colour-coded map after applying a threshold of 2 µm on $C_M(i)_{\mathrm{mean}}$. A simple sketch illustrating the operating principle of this routine is represented in Figure 5. For simplicity, only six domains (A1–A6) were shown.

3. Results and discussion

The diagnostic "gold standard" for the evaluation of morphology in biological tissues is represented by histo-pathological examination. The preparation of histological sections entails several long and invasive procedures, including excision, chemical fixation, cutting and staining, thus making histological analysis feasible only for *ex vivo* tissue samples. On the other hand, SHG microscopy does not require sample processing and provides high resolution imaging of corneal lamellae in a label-free modality, thus holding the potential to be implemented *in vivo* for diagnostic purposes. SHG microscopy is able to highlight the morphology of the corneal stroma with high resolution and contrast, as demonstrated in Figure 1, where two SHG images of healthy and keratoconic corneas, acquired with sagittal optical sectioning geometry, are shown. Collagen lamellae are clearly visible in both images, especially at the interface with Bowman's membrane, making the measurement of their inclination easily feasible. In particular, it is evident from these images that the average angle formed by the orientation of sutural lamellae and the direction of the Bowman's membrane is much higher in healthy than in keratoconic corneas. This datum is in agreement with previous observations performed using SHG microscopy for characterizing keratoconus [23, 24]. The angular orientation of sutural lamellae can be quantitatively evaluated by means of FFT analysis, as shown in Figure 2. Considering a region of interest of about 30 μm in thickness below the Bowman's membrane (Figures 2A and 2B), the intensity profile in the FFT image can be used for characterizing anisotropy in the orientation of sutural lamellae (Figures 2C and 2D). In fact, the FFT image corresponding to keratoconus (Figure 2D) is more anisotropic as compared to the FFT image of healthy cornea (Figure 2C). The calculation of the Aspect Ratio of the FFT intensity profile allowed characterizing the anisotropy of the analysed image and hence discriminating between conditions with stromal lamellae parallel or oriented at large angles with respect to the Bowman's membrane. The distributions of the FFT Aspect Ratio (representing image anisotropy) obtained from the analysis of all the examined and analysed ROIs, are summarized in the histogram in Figure 2E. The Aspect Ratio of the FFT profile offers high sensitivity to discriminate between healthy and keratoconic corneas on the basis of the orientation of their sutural lamellae. The obtained average values of the FFT Aspect Ratio for healthy cornea and keratoconus were found to be statistically different at the 0.001 level after a two-sample statistical *t*-test. However, this analysis requires the acquisition of images with sagittal optical sectioning geometry, which is possible only from *ex vivo* samples. Therefore, the advantage offered with respect to standard histo-pathological examination is minimal. A significant step-forward with respect to the current state-of-the-art methods

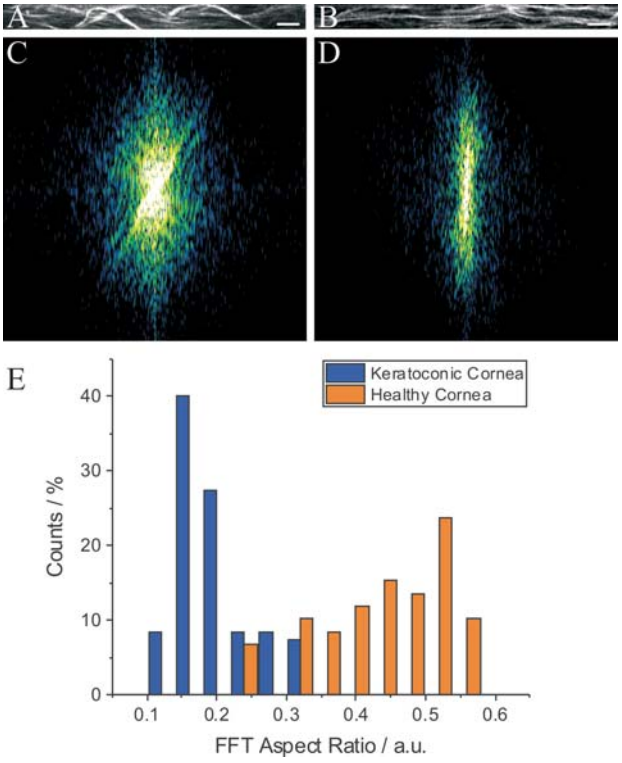

Figure 2 SHG images acquired using sagittal optical sectioning in the first 30 μm below Bowman's membrane (**A**) of a healthy and (**B**) of a keratoconic cornea. Scale bars: 30 μm. (**C**) and (**D**) show FFT of images in (**A**) and (**B**), respectively. (**E**) Histogram distribution of the Aspect Ratio R (ratio between minor and major axes of the FFT intensity profile) calculated on 81 sagittal images of healthy cornea (orange bars) and 97 sagittal images of keratoconic cornea (blue bars). The obtained average values of FFT Aspect Ratio for healthy and keratoconic corneas were found to be statistically different at the 0.001 level after a two-sample statistical *t*-test.

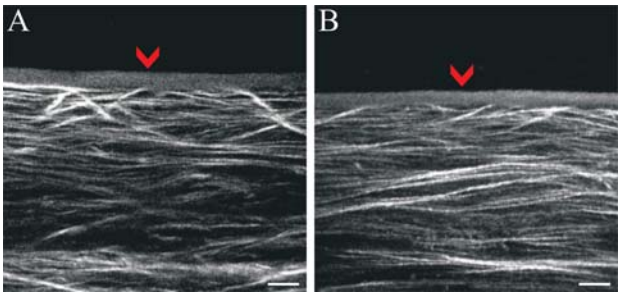

Figure 1 (**A**) SHG image acquired with sagittal optical sectioning of a healthy cornea and (**B**) of keratoconic cornea. The red arrows indicate Bowman's Membrane. Scale bars: 30 μm.

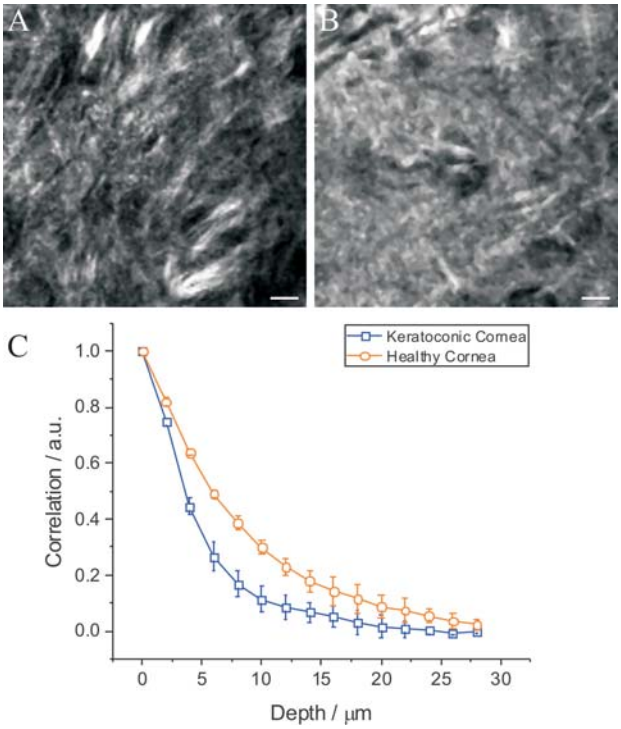

Figure 3 SHG images (**A**) of a healthy cornea, and (**B**) of a keratoconic cornea, acquired with "en-face" optical sectioning and backward detection. Scale bars: 10 μm. (**C**) Average axial Pearson cross-correlation of 10 backward-detected SHG stacks acquired on healthy corneas (orange curve and empty circles) and on keratoconic corneas (blue curve and empty squares).

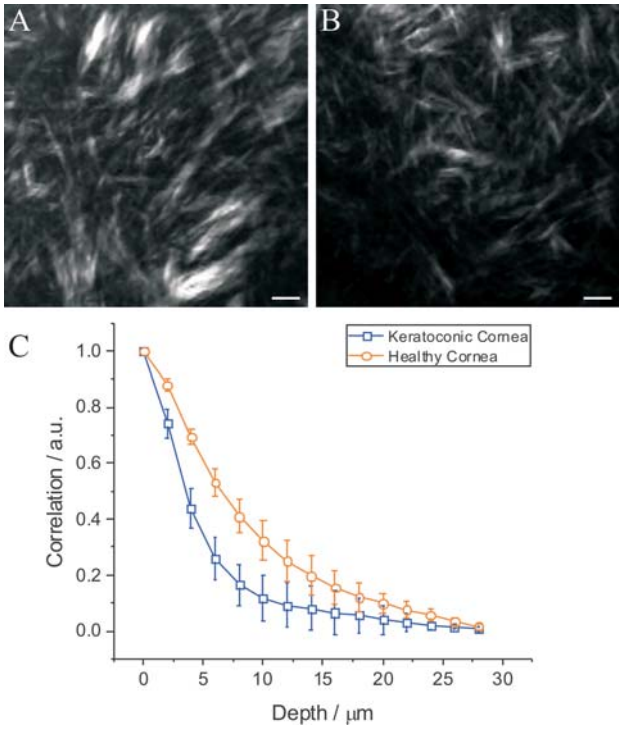

Figure 4 SHG images (**A**) of a healthy cornea, and (**B**) of a keratoconic cornea, acquired with "en-face" optical sectioning and forward detection. Scale bars: 10 μm. (**C**) Average axial Pearson cross-correlation of 10 forward-detected SHG stacks acquired on healthy corneas (orange curve and empty circles) and on keratoconic corneas (blue curve and empty squares).

for diagnosing keratoconus would be the implementation of a method for measuring the orientation of sutural lamellae using "en-face" optical sectioning in combination with epi-detection. Such a method would be extremely powerful for clinical ophthalmic diagnostics.

In order to verify the feasibility of this concept, SHG image stacks were acquired using "en-face" optical sectioning geometry and epi-detection from both healthy and keratoconic samples (Figures 3A, 3B). For the sake of comparison, the same image stacks were simultaneously acquired using also forward-scattered SHG detection with "en-face" optical sectioning geometry (Figures 4A, B) and with sagittal optical sectioning geometry. Considering the different average inclination of sutural lamellae observed in healthy and keratoconic corneas using sagittal optical sectioning geometry, a cross-correlation analysis performed in the direction perpendicular to the corneal surface, may allow characterizing the orientation of sutural lamellae and hence discriminating between healthy and keratoconic samples [36]. For this reason, the Pearson cross-correlation was calculated along the optical axis from stacks of both backward-detected and forward-detected SHG images. The Pearson axial cross-correlation analysis included 10 stacks acquired from healthy corneas and 10 stacks acquired from keratoconic corneas. The calculated Pearson cross-correlation decays were averaged over all examined stacks in order to obtain the curves shown in Figures 3C and 4C for backward-scattered SHG and forward-scattered SHG, respectively. The standard deviations of the values were taken as error bars at each depth. It is important to note that, although the forward-scattered SHG signal is always stronger than the backward-scattered SHG signal because of phase-matching conditions, as demonstrated by the higher contrast in Figures 4A and 4B with respect to Figures 3A and 3B, an excellent agreement was found between the analyses carried out on backward-scattered SHG and on forward-scattered SHG. In particular, the typical length of Pearson axial cross-correlation was found similar for forward- and backward-scattered SHG, as demonstrated by the graphs in Figures 3C and 4C, indicating that the orientation of sutural lamellae can be determined using both backward- and forward-scattered SHG detection. Further, the differ-

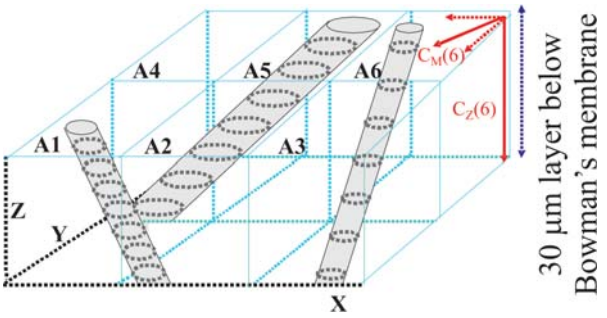

Figure 5 A simple sketch showing the principle behind the method for calculating the inclination of sutural lamellae on the basis of a three-dimensional cross-correlation method.

ence between keratoconic and healthy corneas in terms of cross-correlation decay was significant in each individual region included in the analysis [37]. Considering the fact that this analysis can be successfully implemented also on epi-detected SHG images, acquired using "en-face" optical sectioning geometry, this methodology offers the potential to be used for *in vivo* diagnostics of keratoconus in ophthalmology.

Based on the promising result obtained with Pearson cross-correlation analysis along the optical axis direction, the cross-correlation analysis was extended to all the three spatial directions by calculating the Pearson cross-correlation also in a radial plane. In particular, each SHG image stack was divided into domains of $20 \times 20 \times 30\ \mu m^3$ size. Both axial and radial Pearson cross-correlation were calculated and analysed in each domain, in order to obtain the corresponding typical half-decay lengths $C_Z(i)$ and $C_M(i)_{mean}$ for axial and radial Pearson cross-correlation, respectively. Then, the ratio between $C_Z(i)$ and $C_M(i)_{mean}$ (as defined in Eq. (1)) was taken as a parameter indicating the average lamellar inclination with respect to the Bowman's membrane within each domain. By considering the average angular orientation obtained on all the analysed domains, maps of the orientation of sutural lamellae can be realized, as in Figure 6G, where an example of orientation map for sutural lamellae is shown.

In order to verify the goodness of this three-dimensional Pearson cross-correlation methodology for determining average lamellar orientation, two specific corneal lamellae were identified from SHG stacks acquired using "en-face" optical sectioning and used as target. The average orientation angle of these two specific lamellae was calculated using the three-dimensional Pearson cross-correlation approach (on both backward- and forward-detected SHG stacks). The obtained values were compared to the value obtained by directly measuring the inclination of lamellae from images of the same region acquired with sagittal optical sectioning. The region containing the two specific lamellae was identified in both optical sectioning geometries by means of two marks burned in the corneal epithelium using laser ablation. The region of interest described above, acquired using "en-face" optical sectioning geometry, is shown in Figure 6A and B for forward- and backward-detected SHG, respectively. As in previous acquisitions, even if the contrast is higher for for-

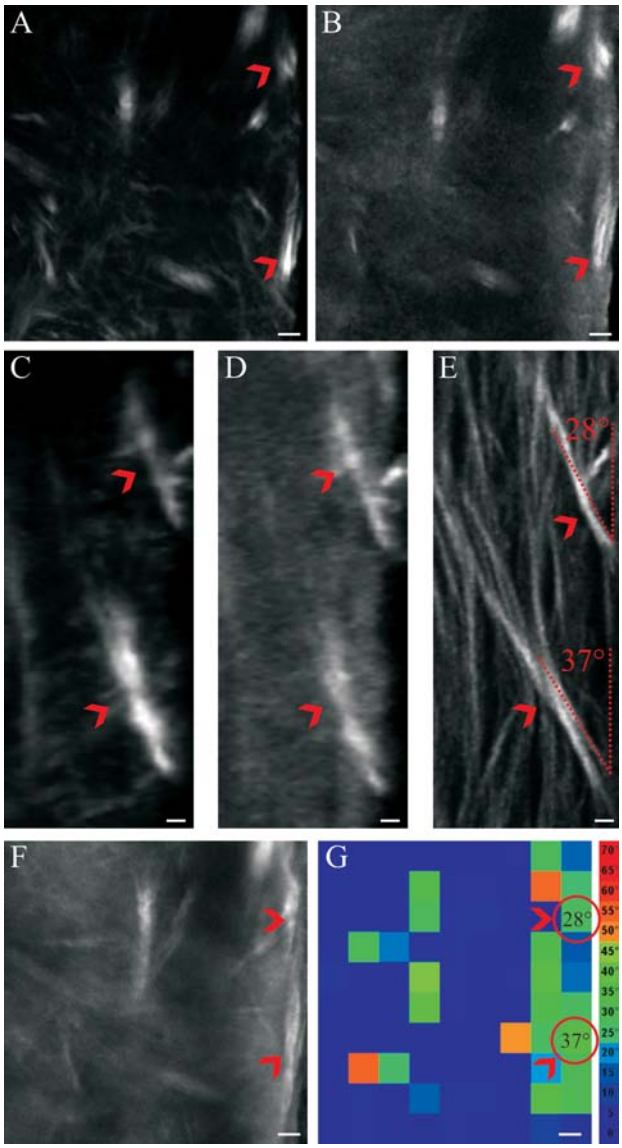

Figure 6 SHG images of a healthy cornea, acquired using "en-face" optical sectioning and forward- (**A**), or backward- (**B**) detection. (**C**) and (**D**) Axial reconstructions (Orthogonal Views plugin, ImageJ) obtained from stacks as those represented in (**A**) and (**B**). (**E**) SHG image of the same area acquired with sagittal optical sectioning. (**F**) Maximum axial intensity projection of a stack acquired in the first 30 μm below Bowman's membrane using "en-face" optical sectioning and backward detection. (**G**) Angular orientation map of sutural lamellae corresponding to the stack shown in (**F**). Scale bars: 10 μm. The red arrows always indicate two specific corneal lamellae.

ward-scattered images, the agreement between backward- and forward-detected SHG images was always good. The corresponding axial projection images, obtained after re-slicing from the SHG stacks acquired with "en-face" optical sectioning geometry (using the "Orthogonal Views" plugin in ImageJ), are represented in Figure 6C and 6D for forward- and backward-detected SHG, respectively. The same region of interest, imaged using sagittal optical sectioning, is depicted in Figure 6E. The agreement among Figures 6C–E is quite good, demonstrating that the morphological features of corneal lamellae can be evidenced not only using sagittal optical sectioning but also using "en-face" optical sectioning. A maximum intensity projection image of the backward-detected SHG stack is depicted in Figure 6F, with the purpose to of representing the whole acquired volume of $120 \times 120 \times 30\ \mu m^3$ below the Bowman's membrane. In all the images presented in Figure 6, the red arrows indicate the two specific lamellae considered for evaluating the three-dimensional Pearson cross-correlation methodology. The two identified lamellae are peculiar in terms of shape and they can be easily identified in "en-face" SHG images (Figures 6A and 6B), in axial reconstruction (Figure 6C and 6D) and in the sagittal SHG image (Figure 6E). A direct measurement of their inclination can be performed using the sagittal optically sectioned image, as shown by the dashed red lines in Figure 6E. The measured orientations were found to be 28° for the upper lamella and 37° for the lamella at the bottom. The method for angular inclination mapping of sutural lamellae, described in Materials and Methods, implemented on epi-detected SHG stacks acquired with "en-face" optical sectioning, gave the result shown in Figure 6G. The angles with respect to the Bowman's membrane in the two domains corresponding to the two identified lamellae were found to be 28° for the upper lamella and 37° for the lower lamella. Hence, an excellent agreement was found between the angles calculated with the proposed method from SHG stacks acquired with epi-detection and "en-face" optical sectioning, and those measured directly from images acquired with sagittal sectioning. In conclusion, the proposed methodology is suitable to probe the average inclination of sutural lamellae within the first 30 μm of corneal stroma below the Bowman's membrane, starting from epi-detected SHG images acquired with "en-face" optical sectioning geometry.

In order to verify the capability of the method for the discrimination between healthy and keratoconic samples on a statistically relevant set of images, inclination maps of sutural lamellae were calculated from 20 SHG stacks acquired in healthy samples and 26 SHG stacks acquired in keratoconic samples. Examples of these sutural lamellae inclination maps are shown in Figures 7B and 7D for a healthy and for a keratoconic sample, respectively. The inclination angles, calculated on all the acquired stacks and on all the analysed domains, are reported in the histogram in Figure 7E for both healthy (orange bars) and keratoconic (blue bars) corneas. The analysis confirmed the fact that sutural lamellae are oriented at smaller angles with respect to the Bowman's membrane in keratoconus, as compared to lamellae oriented at larger angles in healthy cornea. The obtained average values of inclination angle for healthy cornea and keratoconus were found to be statistically different at the 0.001 level after a two-sample statistical

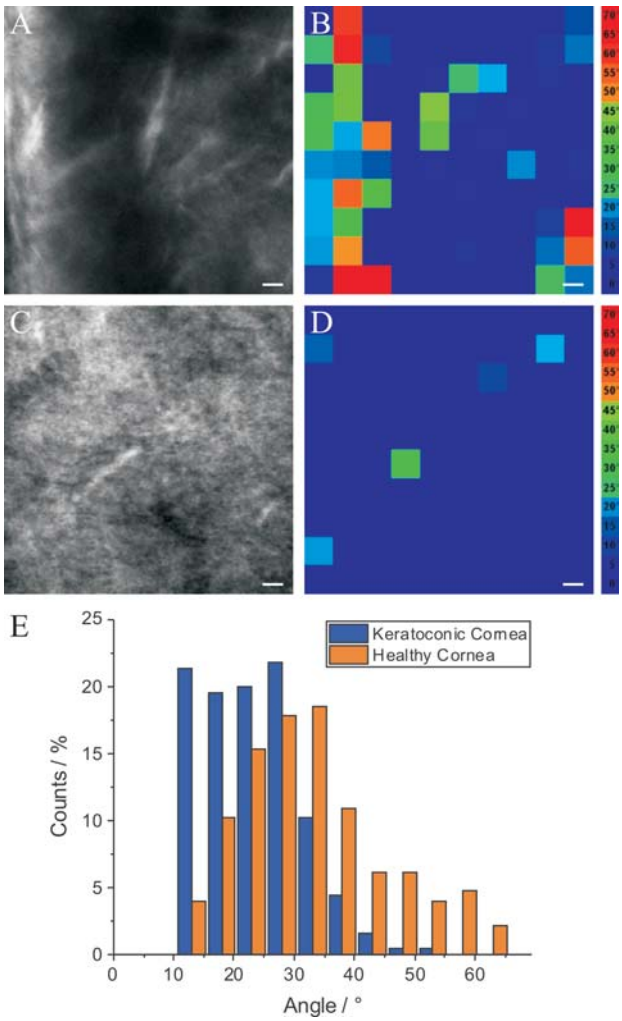

Figure 7 Maximum axial intensity projections from SHG stacks acquired using "en-face" optical sectioning and backward detection from the first 30 μm below Bowman's membrane in healthy cornea (**A**) and in keratoconic cornea (**C**). The corresponding angular orientation maps are represented in (**B**) and (**D**), respectively. Scale bars: 10 μm. (**E**) Histogram of the mean angular orientation distributions of sutural lamellae on all the analysed domains on healthy (orange bars) and keratoconic (blue bars) samples. Angles smaller than 10° are not included in the graph.

t-test. Hence, the proposed methodology holds the promise to provide a very high sensitivity which could be used to diagnose keratoconus at a very early stage. Particularly relevant for clinical diagnostic purposes is the fact that the lamellar orientation can be assessed using an optical configuration scheme that is suitable for *in vivo* imaging in clinical ophthalmic applications.

4. Conclusion

In conclusion, we demonstrated that SHG microscopy can be used for the diagnosis of keratoconus with an optical configuration suitable for *in vivo* ophthalmic imaging. In particular, by using SHG microscopy in combination with a three-dimensional Pearson cross-correlation analysis, it was possible measuring the inclination of sutural lamellae in the anterior part of the corneal stroma, thus discriminating keratoconic from healthy corneas on the basis of this morphological parameter. The presented approach was proven using "en-face" optical sectioning in combination with epi-detection and compared to the direct measurement of lamellar inclination from images acquired using sagittal optical sectioning. This opens the way for a potential *in vivo* use of this methodology for clinical diagnostic purposes. In particular, the reconstruction of lamellar inclination maps from image stacks taken with "en-face" optical sectioning and epi-detection might be suitable for an immediate clinical penetration in the context of ophthalmic diagnostics.

Acknowledgements The research leading to these results has received funding from Tuscany Region and EU FP7 BiophotonicsPlus projects "LITE" (Laser Imaging of The Eye) and "LighTPatcH" (Led Technology in Photo Haemostasis), from the Italian Ministry for Education, University and Research in the framework of the Flagship Project NANOMAX, from the Italian Ministry of Health (GR-2011-02349626), from the European Union Seventh Framework Programme (FP7/2007–2013) under grant agreement number 284464, from Fondazione Pisa and from Ente Cassa di Risparmio di Firenze.

Author biographies Please see Supporting Information online.

References

[1] C. J. R. Sheppard, J. Kompfner, J. Gennaway, and D. Walsh, IEEE J. Quantum Electron **13**, 912 (1977).
[2] W. Denk, H. J. Strickler, and W. W. Webb, Science **248**, 73–76 (1990).
[3] W. R. Zipfel, R. M. Williams, and W. W. Webb, Nat. Biotechnol. **21**(11), 1369–1377 (2003).
[4] R. Cicchi, N. Vogler, D. Kapsokalyvas, B. Dietzek, J. Popp, and F. S. Pavone, J. Biophoton. **6**(2), 129–142 (2013).
[5] F. Helmchen and W. Denk, Nat. Methods **2**(12), 932–940 (2005).
[6] J. Condeelis and J. E. Segall, Nat. Rev. Cancer **3**, 921–930 (2003).
[7] M. J. Levene, D. A. Dombeck, K. A. Kasischke, R. P. Molloy, and W. W. Webb, J. Neurophysiol. **91**(4), 1904–1912 (2004).
[8] P. J. Campagnola, A. C. Millard, M. Terasaki, P. E. Hoppe, C. J. Malone, and A. Mohler, Biophys. J. **81**(1), 493–508 (2002).
[9] S. Psilodimitrakopoulos, V. Petegnief, G. Soria, I. Amat-Roldan, D. Artigas, A. M. Planas, and P. Loza-Alvarez, Opt. Express **17**(16), 14418–14425 (2009).
[10] W. Mohler, A. C Millard, and P. J. Campagnola, Biophys. J. **29**(1), 97–109 (2003).
[11] V. Nucciotti, C. Stringari, L. Sacconi, F. Vanzi, L. Fusi, M. Linari, G. Piazzesi, V. Lombardi, and F. S. Pavone, Proceed. Natl. Acad. Sci. USA **107**(17), 7763–7768 (2010).
[12] D. A. Dombeck, K. A. Kasischke, H. D. Vishwasrao, M. Ingelsson, B. T. Hyman, and W. W. Webb, Proceed. Natl. Acad. Sci. USA **100**(12), 7081–7086 (2003).
[13] I. Freund, M. Deutsch, and A. Sprecher, Biophys. J. **50**(4), 693–712 (1986).
[14] F. Legare, C. Pfeffer, and B. R. Olsen, Biophys. J. **93**(4), 1312–1320 (2007).
[15] A. T. Yeh, N. Nassif, A. Zoumi, and B. J. Tromberg, Opt. Lett. **27**(23), 2082–2084 (2002).
[16] M. Han, G. Giese, and J. F. Billé, Opt. Express **13**(15), 5791–5797 (2005).
[17] W. Radner and R. Mallinger, Invest. Ophthalmol. Vis. Sci. **21**(6), 598–601 (2002).
[18] C. M. Hsheh, W. Lo, W. C. Chen, V. A. Hovhannisyan, G. Y. Liu, S. S. Wang, H. Y. Tan, and C. Y. Dong, Biophys. J. **97**(4), 1198–1205 (2009).
[19] G. Latour, I. Gusachenko, L. Kowalczuk, I. Lamarre, and M. C. Shanne-Klein, Biomed. Opt. Express **3**(1), 1–15 (2012).
[20] W. Lo, W. L Chen, C. M. Hsueh, A. A. Ghazaryan, S. J. Chen, D. Hui-Kang Ma, C. Y. Dong, and H. Y. Tan, Invest. Ophthalmol. Vis. Sci. **53**(7), 3501–3507 (2012).
[21] P. Matteini, F. Ratto, F. Rossi, R. Cicchi, C. Stringari, D. Kapsokalyvas, F. S. Pavone, and R. Pini, Opt. Express **17**(6), 4868–4878 (2009).
[22] P. Matteini, R. Cicchi, F. Ratto, D. Kapsokalyvas, F. Rossi, M. de Angelis, F. S. Pavone, and R. Pini, Biophys. J. **103**(6), 1179–1187 (2012).
[23] Y. Mega, M. Robitaille, R. Zareian, J. McLean, J. Ruberti, and C. DiMarzio, Opt. Lett. **37**, 3312–3314 (2012).
[24] M. Lombardo, D. Merino, P. Loza-Alvarez, and G. Lombardo, Biomed. Opt. Exp. **6**, 2803–2818 (2015).
[25] N. Morishige, W. M. Petroll, T. Nishida, M. C. Kennedy, and J. V. Jester, J. Cataract. Refract. Surg. **32**(11), 1784–1791 (2006).

[26] N. Morishige, Y. Takagi, T. Chicama, A. Takahara, and T. Nishida, Invest. Ophthalmol. Vis. Sci. **52**(2), 1784–1791 (2011).
[27] S. J. Petsche and P. M. Pinsky, Biomech. Model. Mechanobiol. **12**(6), 1101–1113 (2013).
[28] A. Abass, S. Hayes, N. White, T. Sorensen, and K. M. Meek, J. R. Soc. Interface **12**(104), 1–13 (2015).
[29] R. Ambekar, K. C. Toussaint, and A. W. Johnson, J. Mech. Behav. Biomed. Mater. **4**(3), 223–236 (2011).
[30] N. Morishige, R. Shingyouuchi, H. Azumi, H. Ohta, Y. Morita, N. Yamada, K. Kimura, A. Takahara, and K. H. Sonoda, Invest. Ophthalmol. Vis. Sci. **55**, 8377–8385 (2014).
[31] M. Winkler, D. Chai, S. Kriling, C. J. Nien, D. J. Brown, B. Jester, T. Juhasz, and J. V. Jester, Invest. Ophthalmol. Vis. Sci. **52**, 8818–8827 (2011).
[32] M. Winkler, G. Shoa, Y. Xie, S. J. Petsche, P. M. Pinsky, T. Juhasz, D. J. Brown, and J. V. Jester, Invest. Ophthalmol. Vis. Sci. **54**, 7293–7301 (2013).
[33] F. Rossi, A. Canovetti, A. Malandrini, I. Lenzetti, R. Pini, and L. Menabuoni, J. Vis. Exp. **101**, e52939 (2015).
[34] A. Canovetti, A. Malandrini, I. Lenzetti, F. Rossi, R. Pini, and L. Menabuoni, Am. J. Ophthalmol. **158**(4), 664–670 (2014).
[35] R. Cicchi, D. Kapsokalyvas, V. De Giorgi, V. Maio, A. Van Wiechen, D. Massi, T. Lotti, and F. S. Pavone, J. Biophoton. **3**, 34–43 (2010).
[36] G. Chinga and K. Syverud, Nord. Pulp. Pap. Res. **22**(4), 441–446 (2007).
[37] R. Mercatelli, F. Ratto, F. Tatini, F. Rossi, L. Menabuoni, R. Nicoletti, R. Pini, F. S. Pavone, and R. Cicchi, Proceed. SPIE **9693**, Ophthalmic Technologies XXVI, 96930Y (2016).